

TRAJECTORIES FOR A NEAR TERM MISSION TO THE INTERSTELLAR MEDIUM

Nitin Arora,* Nathan Strange,† and Leon Alkalai‡

Trajectories for rapid access to the interstellar medium (ISM) with a Kuiper Belt Object (KBO) flyby, launching between 2022 and 2030, are described. An impulsive-patched-conic broad search algorithm combined with a local optimizer is used for the trajectory computations. Two classes of trajectories, (1) with a powered Jupiter flyby and (2) with a perihelion maneuver, are studied and compared. Planetary flybys combined with leveraging maneuvers reduce launch C_3 requirements (by factor of 2 or more) and help satisfy mission-phasing constraints. Low launch C_3 combined with leveraging and a perihelion maneuver is found to be enabling for a near-term potential mission to the ISM.

INTRODUCTION

In September 2013, Voyager-1 Project Scientist Dr. Edward C. Stone announced that the craft had entered interstellar space in August 2012.¹ In July 2015,² the New Horizons spacecraft flew by Pluto, passing a major milestone in space exploration. Meanwhile, the Kepler Space Telescope, on its mission to find planets around other stars, has yielded spectacular results including detection of Earth-like planets in our galactic neighborhood.³ These events bring the emerging area of Interstellar Medium (ISM) exploration into focus, provoking the question: “*What is humanity’s next step, as it ventures out into interstellar space, toward another star?*”

To answer these questions, Caltech’s Keck Institute for Space Studies (KISS) sponsored two workshops⁴ on the topic of the Science and Enabling Technologies for the Exploration of the Interstellar Medium (ISM), led by Dr. Edward C. Stone (Caltech), Dr. Leon Alkalai (JPL), and Louis Friedman (The Planetary Society, Co-Founder and Executive Director Emeritus).⁵ The two workshops made it clear that a near-term robotic mission to the ISM^{6,7} would generate science compelling to a number of disciplines, particularly Heliophysics, Astrophysics, and Planetary Science.

The KISS workshop team endorsed the ambitious goal of traveling faster and reaching the ISM in a much shorter time frame than Voyager. Taking advantage of a rare planetary alignment, the Voyager spacecraft performed multiple outer planet flybys and is currently escaping our solar system at a speed of ~ 17 km/s. Even so, the spacecraft took ~ 38 years (since its launch in 1977) to reach a distance of 132 AU (as of August 2015) from the Sun. Traveling many times faster than Voyager would not only bring the otherwise distant local ISM (150–200 AU) science much closer to home, but would also enable rapid exploration of the pristine ISM (>200 AU). In addition, the workshop team identified a large Kuiper Belt Object (KBO) flyby as one of the primary goals of the mission as opposed to being an afterthought, as it was on New Horizons.

Trajectories for escaping the solar system have been studied since the 1970s.^{8,9,10} One of the conclusions of a 1975 NASA interstellar flight study was to launch a small spacecraft (in 1980s) using electric propulsion, solar sails, and/or Jupiter flyby to reduce the flight time to the heliospheric boundary. Since then, there have been a plethora of mission studies on the topic of fast solar system escape. Previous studies have identified trajectories utilizing Jupiter swing-by and/or maneuvers close to the Sun in combination with Solar Sails,^{11,12}

*Jet Propulsion Laboratory, California Institute of Technology, Nitin.Arora@jpl.nasa.gov, 818-354-2417

†Jet Propulsion Laboratory, California Institute of Technology, Nathan.J.Strange@jpl.nasa.gov

‡Jet Propulsion Laboratory, California Institute of Technology, leon.alkalai@jpl.nasa.gov

electric propulsion,^{12,13} or both.^{12,14,15} Propulsion using nuclear pulsed detonation (under Project Orion) was also studied in late 1960s.¹⁶ An innovative solar thermal propulsion combined with a perihelion maneuver was also studied as part of a step 2 NIAC.¹⁷ Later, a Radioisotope Electric Propulsion (REP) based approach (with a Jupiter gravity assist) was developed (known in literature as the “Innovative Interstellar Explorer”) which had considerably less mass than spacecraft envisioned in earlier studies.^{13,18} During the same time, the European Space Agency (ESA) spent a long time investigating a solar-sails–based Heliopause Explorer concept.^{19,20} Later in 2009/2010, a hybrid mission concept, “the Interstellar Heliopause Probe/Heliospheric Explorer,” was proposed.²¹ Recently, use of the Space Launch System (SLS) for enabling an interstellar probe mission was also investigated.²² Most of the previous studies have focused primarily on escaping the solar system and did not target a specific escape direction or a KBO. Furthermore, the trajectories used in these previous studies require launching from Earth with high launch energies, or C_3 s ($> 80 \text{ km}^2/\text{s}^2$), which severely limits total spacecraft mass (including on-board propulsion capabilities). A dramatic reduction in launch C_3 (at the expense of a modest increase in flight time) can be achieved by performing inner-planet gravity assists before escaping the solar system. A similar reduction in C_3 was identified in a previous design study (from 1995²³), which envisioned delivering a small (200 kg) probe to the ISM (without a KBO flyby), launching in the early 2000s.

In this paper, a large set of trajectories for a notional near-term mission (launching between 2022 and 2030) to the ISM with a KBO flyby are identified and documented. The solution approach consists of a broad search followed by local pruning and optimization. An impulsive-patched-conic–based search algorithm (called Star), capable of adding optimal powered flybys and impulsive leveraging maneuvers between flybys, is used for the initial broad search. Potential mission goals and constraints are then used to further prune the solution space. A subset of the remaining large set (up to ~ 8 million) trajectories is then refined using Mission Analysis Low-Thrust Optimization (MALTO), JPL’s discrete trajectory optimizer. Julia, a new high-performance computing language, is used as the main driver layer for controlling execution and flow of data between the two tools.

Two major classes of trajectory are studied: 1) trajectories with a powered Jupiter flyby and 2) trajectories with a perihelion ΔV (impulsive maneuver close to the Sun). For both classes, key trajectory trades based on launch C_3 , flight time, solar system escape velocity (V_∞^{sun}), choice of gravity assist bodies, choice of KBO flybys, and ΔV requirements are presented. The KBO flyby requirement imposes a phasing constraint on the trajectory, thereby pruning a significant portion of design space. The effect of powered flybys and a leveraging deep space maneuver (DSM) between flybys is also quantified. In most cases a leveraging DSM is found to benefit mission performance by reducing flight time or launch C_3 , and/or by improving the phasing.

We start by defining problem goals, assumptions, and constraints. Next, we study the characteristics of two trajectory classes, followed by a detailed trade space exploration and identification of high performing trajectories for near-term exploration of the ISM.

PROBLEM DEFINITION

Motivated by the goals set by the KISS workshop team, trajectories for a near-term mission to the ISM need to satisfy the following four design goals:

1. Launch within the next decade; between 2022 and 2030;
2. Reach the local ISM (180 AU–200 AU) in ~ 20 years from launch;
3. Travel into the ISM with an solar system escape velocity (V_∞^{sun}) $> 13 \text{ AU/yr}$ (compared to Voyager 1’s $\sim 3.6 \text{ AU/yr}$ and New Horizon’s $\sim 2.5 \text{ AU/yr}$); and
4. Perform a flyby of a large KBO.

It should be noted that, though generally true, goals 2 and 3 are not always synergistic with each other. For example, a spacecraft can trade time of flight and maximize its V_∞^{sun} by performing multiple gravity assists before escaping the solar system or it may perform a single Jupiter flyby, resulting in a quicker access to the

near ISM (~ 100 AU) but with a lower solar system escape velocity. Furthermore, targeting a KBO enforces inclination and phasing constraints on the trajectory, which limits possible launch dates and results in a non-linear design space. Other key trade space parameters from a spacecraft design and mission architecture perspective are: launch energy (C_3), minimum distance from the Sun (perihelion), total trajectory ΔV , and time of flight (TOF) to the KBO.

KBO Targets

The Kuiper belt is a disc-shaped region beyond the orbit of Neptune, extending all the way to 50 AU. As of August 2015, more than 100,000 KBOs over 50 km in radius are believed to exist. Table 1 lists the largest known KBOs (excluding Pluto) along with their mass / orbital characteristics, corresponding to epoch of August 1, 2035.

Table 1. List of large KBOs (epoch = August 1st, 2035; observer = Sun; frame = Ecliptic, J2000)

| KBO Name | Mean radius (km) | Radial distance (AU) | Lat (deg.) | Lon (deg.) | Mission target |
|-------------------------|------------------|----------------------|------------|------------|----------------|
| Eris | 1,163 | 95 | -8.6 | 26.9 | N |
| MakeMake | 715 | 53 | 25.5 | 200.1 | Y |
| 2007 OR ₁₀ * | 640 | 91.7 | 0.7 | 337.9 | N |
| Haumea | 620 | 49 | 27.8 | 222.9 | Y |
| Quaoar | 555 | 42 | 7.7 | 293.3 | Y |
| Sedna | 498 | 81 | -11.6 | 67.2 | N |
| Orcus | 425 | 48 | -20.6 | 176.6 | Y |

The trajectory for a mission to the ISM should aim for the nose of the heliosphere, a direction that provides the shortest route to the local ISM. Traveling toward the nose also benefits studies of the in-flowing interstellar plasma and neutral particle populations.^{24,25,26} The nose of the heliosphere is currently known to have a latitude and longitude of 7.5° and 245.5° , respectively. Hence, selected KBO targets that are not close to the nose of the heliosphere are not fruitful and are not considered in this study. Furthermore, KBOs which are beyond 60 AU in a decade from launch (~ 2035) are also not considered. Applying these two criteria, the final list of selected KBO targets consists of: Haumea, MakeMake, Quaoar, and Orcus. Given the recent New Horizons flyby of Pluto, it is not considered as a target for the ISM mission in this work.

Propulsion Options

1. Impulsive: The focus of this study is primarily on impulsive (high thrust) trajectories with leveraging DSMs, perihelion maneuvers, and powered flybys. Based on a JPL Team-X carried out in September 2014, and assuming advances in power system technology in the next ten years, the mass (M_p) of the ISM probe is optimistically assumed to be ~ 300 kg. Assuming a Centaur²⁷ propulsive stage (Fuel mass = 20,830 kg, Dry mass = 2,247 kg, $I_{SP} = 450.5$ sec), the maximum allowable spacecraft ΔV is calculated to be ~ 9.8 km/sec.

In this work we assume a total ΔV of 10 km/sec for trajectories with perihelion > 0.15 AU and a total ΔV of 8 km/sec for trajectories with perihelion < 0.15 AU. The reduction in ΔV accounts for the heat shield mass required to get close to the Sun. Furthermore, based on analysis carried out at JPL in September 2014, the minimum perihelion distance possible with current state-of-the art heat shield technology is found to be 2.8 solar radii (from the center of the Sun). Detailed discussions on the spacecraft flight system is beyond the scope of this paper and will be addressed in other complementary articles.

2. Low Thrust: Low-thrust trajectories (both nuclear and solar powered) are not considered in this study and will be a subject of future work.

3. Solar sails: In this paper we limit ourselves to trajectories in which the solar sail is deployed on the escape phase of the trajectory. In other words, the sail is only used to increase spacecraft V_∞^{sun} and radial distance (relative to the Sun) after 20 years.

The main parameter affecting solar sail performance is called sail loading and is defined as follows:

$$\text{sail loading} = \frac{M_p}{A} \quad (1)$$

where M_p is the mass of the ISM probe in kg and A is the effective sail area in m^2 . Hence, the acceleration on the spacecraft due to solar pressure is inversely proportional to sail loading. Table 2 lists sail loading of NASA missions that are currently under development or recently canceled.

Table 2. Sail loading of selected solar sail missions

| Mission Name | A (m^2) | sail loading (g/m^2) |
|--------------|----------------------|--|
| Sunjammer | 1,200 | 26.7 |
| NEAScout | 83 | 144.6 |
| Lightsail | 32 | 156.3 |
| IKAROS | 196 | 1,607 |

In this study, three sail loading values of $20 \text{ g}/\text{m}^2$, $15 \text{ g}/\text{m}^2$, and $10 \text{ g}/\text{m}^2$, corresponding to low, medium, and high development risk, are considered. Note that for an ISM probe of mass 300 kg, a sail loading of $10 \text{ g}/\text{m}^2$ results in a sail area of $30,000 \text{ m}^2$.

TRAJECTORY DEFINITION

Two classes of trajectories are considered in this study. Type 1 trajectories, which rely on a powered Jupiter flyby to get the required change in velocity, and type 2 trajectories, which rely on a impulsive maneuver very close to the Sun. Maneuvers at the perihelion (closest point to the Sun) and at the perijove (closest point during Jupiter flyby) take advantage of the well-known Oberth effect,²⁸ which states that the efficiency of a propulsive maneuver is proportional to the speed of the spacecraft. This effect is directly proportional to the mass of the gravitational body and the distance from its center. Characteristics of the two class of trajectories are discussed below.

Type 1: Trajectories with a powered Jupiter flyby

Figure 1 shows a notional type 1 trajectory. The trajectory can be broken down into three phases:

1. Energy build-up phase: In this phase, the spacecraft increases its orbital energy and achieves required phasing (for targeting a KBO post-Jupiter flyby). The energy build phase may involve a combination of multiple inner solar system gravity assists and DSMs (for targeting, leveraging, or plane change).

2. Powered flyby phase: In this phase, the spacecraft approaches Jupiter on a hyperbolic trajectory (relative to the planet), performs a ΔV at or near the perijove (Oberth maneuver²⁸), and escapes the Jupiter planetary system at significantly higher V_∞^{Jup} . In the frame centered at the Sun, this results in a powered gravity assist at Jupiter, resulting in a large increase in spacecraft V_∞^{sun} . The Jupiter flyby is also used for targeting the KBO on the escape leg.

3. Escape phase: In this phase, the spacecraft escapes the solar system, performing a fast KBO flyby and scientific observations as it ventures deep into the local ISM.

In this paper, type 1 trajectories with up to three flybys (including Jupiter) are considered during the broad search. Furthermore, DSMs are considered only during the energy build-up phase of the trajectory. The minimum permissible powered flyby altitude at Jupiter is 3,000 km.

Type 2: Trajectories with a Perihelion Maneuver

Figure 2 shows a notional type 2 trajectory. The trajectory can be broken down into four phases:

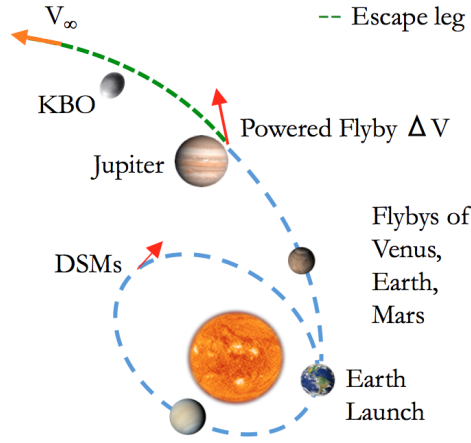


Figure 1. Notional type 1 trajectory with a powered Jupiter flyby

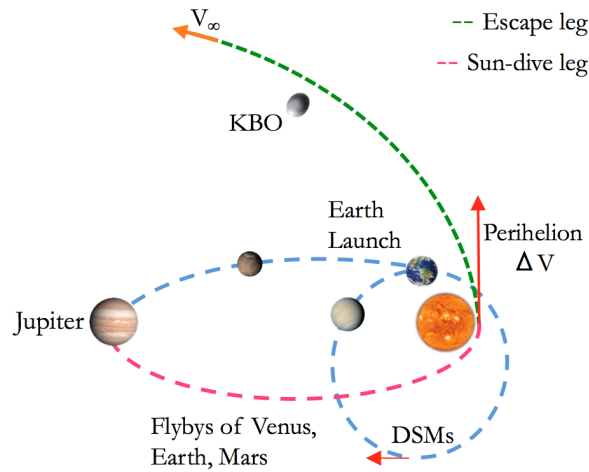


Figure 2. Notional type 2 trajectory with a perihelion maneuver

1. *Energy build-up phase:* This phase is similar to a type 1 trajectory, where the spacecraft increases its energy and achieves required phasing (for targeting a “hair-pin” Jupiter flyby). The energy build phase may involve a combination of multiple inner solar system gravity assists and DSMs (for targeting, leveraging, or plane change).

2. *Sun-dive phase:* In this phase, the spacecraft performs a dramatic Jupiter “hair-pin” gravity assist, putting it on a Sun-dive trajectory. For a given perihelion distance from the Sun, the minimum V_∞^{jup} at Jupiter can be analytically calculated by assuming post-flyby aphelion at Jupiter. Figure 3 shows the minimum V_∞^{jup} as a function of perihelion distance (from center of the Sun). The limiting perihelion distance of 2.8 solar radii requires a V_∞^{jup} of ~ 12.1 km/sec.

3. *Perihelion maneuver phase:* As the spacecraft approaches the perihelion, it performs a ΔV (Oberth maneuver²⁸) which results in a large change in spacecraft energy and hence in V_∞^{sun} . For an optimal type 2 trajectory, the Jupiter flyby does the required plane change for targeting the KBO while the ΔV at perihelion maximizes V_∞^{sun} . For KBOs with relatively high inclination (e.g., MakeMake), this results in a near polar approach to the Sun. To further understand the effect of the perihelion maneuver, Fig. 4 shows V_∞^{sun} contours (in AU/yr) for parametrically varying values of perihelion distance (x-axis) and ΔV executed at perihelion (y-axis). For this plot, the solar approach trajectory is assumed to be parabolic. As expected, the solar system departure V_∞^{sun} increases substantially as the perihelion distance goes down and as the ΔV of the maneuver

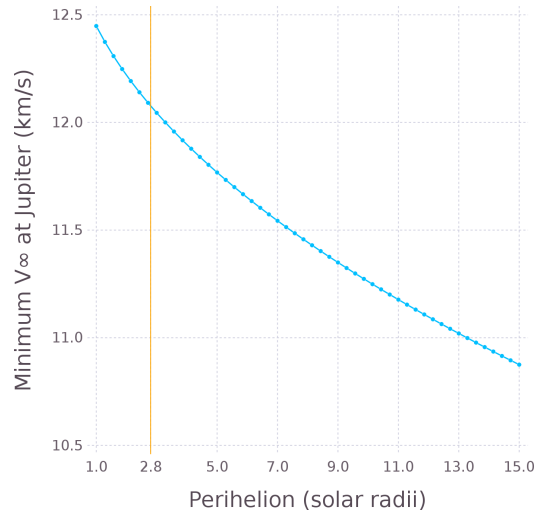


Figure 3. Minimum V_{∞}^{Jup} vs. perihelion distance (solar radii), orange line = heat shield limit

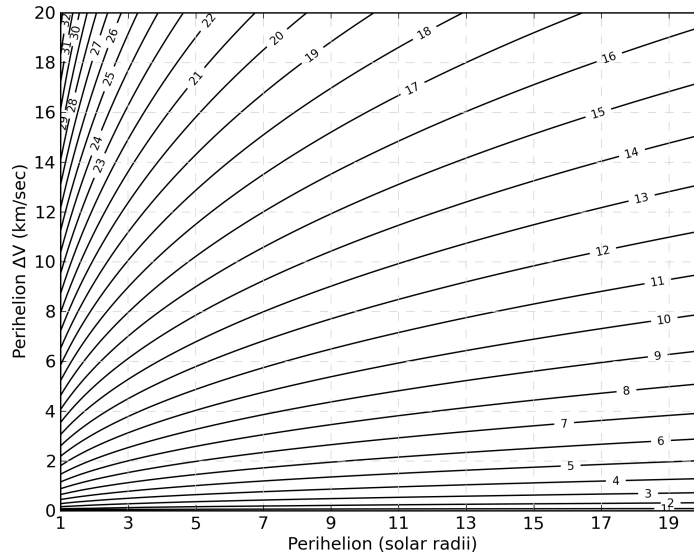


Figure 4. Escape V_{∞}^{sun} contours (AU/yr) for a parabolic solar approach trajectory

goes up. As an example, a 5 km/sec ΔV at a 4 solar radii would result in a V_{∞}^{sun} of ~ 11 AU/yr, a little over 3 times that of Voyager-1. Going as close as 2 solar radii would result in resulting V_{∞}^{sun} of ~ 14 AU/yr, almost 4 times that of Voyager-1.

Regarding such close flybys of the Sun, it should be noted that the currently planned Solar Probe Plus mission is designed for an 8.5 solar radii perihelion.²⁹ The earlier design (called the Solar Probe mission) was designed to achieve a final perihelion of 4 solar radii, i.e., 3 solar radii from the surface.³⁰

4. Escape phase: In this phase the spacecraft escapes the solar system, performing a fast KBO flyby and scientific observations, as it ventures deep into the local ISM. To further increase the escape velocity, a solar sail may be deployed during this phase once the spacecraft reaches to a distance of 0.2 AU from the Sun.

SOLUTION APPROACH

Given the computationally intensive nature of the problem, a multi-step solution approach is adopted. The first step involves a broad search for finding near-feasible trajectories, satisfying various constraints as outlined in previous sections. An impulsive-patched-conic-based search algorithm (implemented in MATLAB, as a tool called Star) is used for searching through a large number (on the order of billions) of possible transfers.

Star is a vectorized, broad trajectory search tool, relying on an algorithm in which the encounter times for the flyby bodies are precomputed based on input time of flight and step size constraints. The algorithm computes various orbital transfers (between flyby bodies) as solutions to the multiple revolution Lambert problem. Unlike other broad search algorithms in literature,^{31,32} which rely on V_∞ matching, Star patches together multiple trajectory arcs with mismatch ΔV s at flybys. Allowing for mismatch, this increases the speed of the search algorithm and results in a larger set of feasible trajectories. The precomputed, discretized TOF grid further enables flyby trajectory arcs to be computed independently, resulting in faster computation times and a net reduction in total number of Lambert function calls. DSM locations between flyby bodies are computed by reducing the problem to a fast, single-variable root solve³³ (using Lawden's primer vector theory³⁴). This capability is utilized for finding leveraging DSMs during the energy build phase and for computing perihelion ΔV for type 2 trajectories. Optimal location of a powered flyby maneuver (used for computing type 1 trajectories) is calculated via a primer vector-based approach, as developed by Gobetz,³⁵ Walton,³⁶ and Hyde.³⁷

The second step involves filtering (for problem-specific constraints) the large set of computed solutions in the previous phase and binning them into families of trajectories having similar launch date (within 30 days of each other), same flyby bodies sequence, and same number of DSMs.

The third step involves optimizing a representative subset of trajectories (typically one from each family) using MALTO³⁸ to check for feasibility. MALTO is JPL's in-house trajectory optimizer for preliminary mission design, capable of optimizing both low thrust and high thrust trajectories. MALTO breaks the trajectory into discretized keplerian segments with an impulsive ΔV in the middle of each segment. This results in a constrained optimization problem, which is then solved using the nonlinear programming software SNOPT. A trajectory is deemed feasible if the flyby ΔV can be optimized below 20 m/s (except for the powered Jupiter flyby in Type 1 trajectories) and the trajectory satisfies the user-supplied V_∞^{sun} , flight time, flyby altitude, ΔV , and KBO targeting constraints. If a trajectory is feasible, then the whole set of trajectories belonging to that same family are assumed to be feasible.

The two software tools (Star and MALTO) are executed via the main driver code, written in Julia (latest stable branch, version 0.3.9). Julia³⁹ is a new, open source, high-level dynamic programming language capable of performance (execution speed) close to (within $2\times$ computation time) that of compiled C or Fortran code. It has syntax similar to other technical computing environments (like MATLAB) and has attractive features like inbuilt parallelism, variable numerical accuracy, attractive plotting capabilities, inbuilt linear algebra libraries (like BLAS, LAPACK, etc.), and tightly integrated high-performance solvers/optimization packages (JuMP, Sundials, Ipopt, KNITRO, etc.). Another major attractive feature is Julia's ability to call Python, C, and Fortran functions and libraries without any wrapper or glue code. This makes it possible to easily leverage existing, optimized implementations of various astrodynamics software in C or Fortran.

RESULTS

In this section, the result from the extensive broad trajectory search are presented. The trade space variables considered in this study are: distance after 20 years (AU), TOF to KBO (years), number of flybys, escape velocity (V_∞^{sun}) (AU/yr), launch C_3 (km^2/sec^2), launch date (yr), Jupiter powered flyby ΔV (km/sec, only for type 1 trajectories), solar perihelion ΔV (km/sec, only for type 2 trajectories), perihelion distance (solar radii, only for type 2 trajectories) and target KBO. Unless otherwise stated, the performance objective for ranking various trajectories is the distance achieved in 20 years from launch. Table 3 lists various input parameters and constraints used in computing these results.

Table 3. Input parameters

| Parameter name | Value |
|---|---------------------------------|
| Launch window (year) | 2022–2030 |
| Maximum TOF to KBO (years) | 15 |
| Minimum V_{∞}^{kbo} at KBO (km/sec) | 35 |
| Maximum launch C_3 (km^2/sec^2) | 15 |
| Minimum perihelion distance (solar radii) | 2.8 |
| Minimum Jupiter powered flyby altitude (km) | 3,000 |
| Maximum total mission ΔV for type 1/2 trajectories (km/sec) | 10/8 |
| Mission KBO targets | MakeMake, Haumea, Quaoar, Orcus |
| Gravity assist bodies | Venus, Earth, Mars, Jupiter |
| Maximum DSM per leg (km/sec) | 1 |
| Maximum Lambert revolutions per leg (energy build up phase) | 2 |
| Maximum number of gravity assists for type 1 trajectories | 3 |
| Maximum number of gravity assists for type 2 trajectories | 4 |

Type 1 trajectories to the ISM

In total, ~ 1.5 million feasible type 1 trajectories are found, out of which 618,172 use one flyby (Jupiter only), 830,521 use two flybys, and 135,375 use three flybys. The inner solar system flyby bodies allowed during the search are either Earth, Venus, or Mars.

Figure 5 shows the trade space for all feasible type 1 trajectories. The trajectories are color coded with the number of flyby bodies. There are five sub-figures corresponding to pairs trade space variables. Each sub-figure is divided in 4 columns, where each column corresponds to one of the target KBOs. The horizontal axis for each sub-figure corresponds to distance from the sun after 20 years' launch. This allows for quick comparison of trajectories across various trade space variables by drawing a vertical line on Fig. 5. One of the first things to note is there are no type 1 trajectories with an $V_{\infty}^{sun} > 11$ AU/yr (even for launch $C_3 > 200$ km^2/s^2). The second thing to note is that only a small set of very high launch C_3 , high ΔV (at Jupiter), one-flyby trajectories reach a distance of 180–200 AU in 20 years. Another interesting aspect to note is that most of the type 1 trajectories (one- and two-flyby case) reach the target KBO in < 10 years. One-, two-, and three-flyby trajectories require a minimum launch C_3 of ~ 76 , ~ 29 and ~ 25 km^2/s^2 , respectively. The performance (in terms of V_{∞}^{sun} and distance achieved in 20 years) decreases with an increased number of flybys. The highest performing trajectories are found for target the KBO Quaoar due its relatively low inclination (see 1) to the ecliptic plane. Launch opportunities exists over the whole 8-year launch window. High performing trajectories to Orcus, MakeMake, Haumea, and Quaoar prefer launch dates around 2024, late 2025, 2026–2027, and 2027–2028, respectively. Table 4 documents various highest-performing type 1 trajectories (in terms of maximum distance achieved) to each target KBO for a range of launch C_3 s.

Table 4. Representative Type 1 Trajectories(unoptimized)

| Case | KBO | Flybys | Launch (month/year) | Flyby Dates (month/year) | KBO TOF (yrs.) | Distance (AU) | V_{∞}^{sun} (AU/Yr.) | C_3 (km^2/s^2) | DSM/leg (km/sec) | Jupiter ΔV (km/sec) |
|--|----------|--------|------------------------|-----------------------------|-------------------|------------------|--------------------------------|---------------------------------------|---------------------|--------------------------------|
| $C_3 \leq 150 \text{ km}^2/\text{s}^2$ | | | | | | | | | | |
| 1 | MakeMake | J | 08/24 | 12/25 | 6.9 | 176 | 9.3 | 123 | 0,0 | 9.8 |
| 2 | Haumea | J | 10/25 | 12/26 | 6.1 | 184 | 9.7 | 148 | 0 | 9.8 |
| 3 | Quaoar | J | 12/28 | 03/30 | 5.3 | 186 | 9.7 | 147 | 0 | 9.8 |
| 4 | Orcus | J | 08/24 | 10/25 | 5.7 | 189 | 9.8 | 149 | 0 | 9.9 |
| $C_3 \leq 100 \text{ km}^2/\text{s}^2$ | | | | | | | | | | |
| 5 | MakeMake | J | 08/24 | 04/25 | 7.1 | 173 | 9.3 | 100 | 0,0 | 9.8 |
| 6 | Haumea | J | 09/25 | 05/27 | 6.8 | 170 | 9.1 | 99 | 0 | 9.8 |
| 7 | Quaoar | J | 11/27 | 07/29 | 6.0 | 176 | 9.4 | 99 | 0 | 9.8 |
| 8 | Orcus | J | 07/23 | 03/25 | 6.8 | 166 | 8.9 | 98 | 0 | 9.8 |
| $C_3 \leq 50 \text{ km}^2/\text{s}^2$ | | | | | | | | | | |
| 9 | MakeMake | E,J | 10/22 | 07/24,05/26 | 9.3 | 148 | 8.8 | 49 | 0,7,0,2 | 8.8 |
| 10 | Haumea | E,J | 11/23 | 08/25,07/27 | 9.4 | 135 | 8 | 44 | 0,7,0,4 | 8.6 |
| 11 | Quaoar | E,J | 01/26 | 10/27,09/29 | 8.1 | 150 | 8.9 | 42 | 0,7,0,5 | 8.6 |
| 12 | Orcus | E,J | 10/22 | 07/24,12/25 | 9.1 | 131 | 7.5 | 36 | 0,9,1 | 8 |

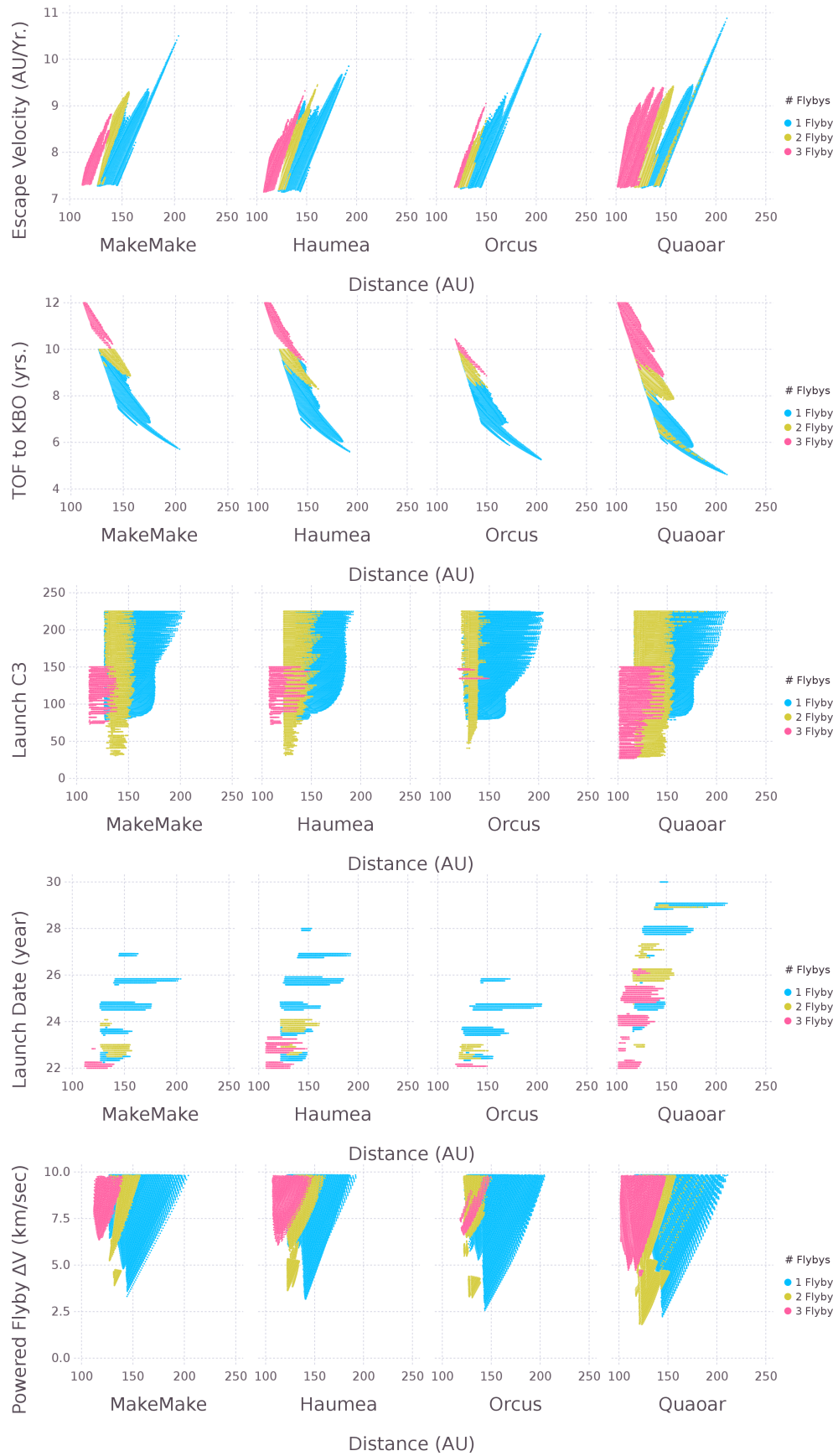


Figure 5. Results: Type 1 Trajectories (up to 3 flybys)

Type 2 trajectories to the ISM

Given the more energetic nature of the general mission design scenario, a large number of type 2 trajectories are found during the step 1 (broad search) of the solution process. After binning and the limited feasibility analysis (via MALTO), a final set of 8,016,878 trajectories are found to be feasible. Compared to type 1 trajectories, these take more time to reach the KBO but are able to reach much larger radial distances due to higher escape velocities.

Figures 6–9 show all type 2 trajectories with one, two, three, and four flybys, respectively. Each figure is divided into various rows (corresponding to different trade space variables). Each sub-figure row is divided by flyby KBO type. The dots on the figures are color-coded by TOF to KBO (in years) values. As in the previous case, the horizontal axis of each sub-figure corresponds to distance achieved in 20 years.

One-flyby trajectories: Figure 6 maps the trade space for type 2 trajectories with a Jupiter flyby (before the perihelion maneuver). One the first thing to notice (in Figure 6) is that there exists a large number of one-flyby (Jupiter only) trajectories to KBOs Haumea and MakeMake, which reach a distance of > 200 AU in 20 years from launch. Another thing to note from Figure 6 is that there are no feasible single-flyby trajectories to Quaoar. Finally, it is also noted that only a small number of lower performing trajectories are found to Orcus.

In terms of launch C_3 requirements, the high performing, single-flyby type 2 trajectories require a minimum C_3 of $\sim 110 \text{ km}^2/\text{sec}^2$. This value is high and may result in unfeasible trajectories when coupled with launch vehicle, spacecraft flight system, and required mission ΔV constraints. Also, as expected, the highest performing cases get as close as 2.8 solar radii from the center of the sun for executing the perihelion maneuver. The maneuver ΔV is found to vary between 5 km/sec to 7 km/sec for high performing cases.

The highest performing cases for MakeMake, Haumea, and Orcus are able to achieve an V_∞^{sun} of ~ 14.2 , 12.7, and 10.7 AU/yr, respectively. Given the complex phasing constraint requirements of the trajectory, only a handful of launch opportunities exist. Trajectories to MakeMake, Haumea, and Orcus are possible in early 2028, early 2029, and early 2028, respectively.

Two-flyby trajectories: Figure 7 maps the trade space for type 2 trajectories with two solar-system flybys. As for all type 2 trajectories, the flyby before the perihelion maneuver is always at Jupiter. In contrast to the one-flyby case, all KBOs are accessible with the two-flyby trajectories. Given the lower C_3 requirements (almost half of what is required for one flyby), the trajectories end up taking more time to reach the KBO.

While achieving similar V_∞^{sun} as the one-flyby case, the trajectories do not cross (but come close) to the 200 AU radial distance limit (in 20 years from launch). The launch C_3 requirements for these trajectories range from 43–64 km^2/sec^2 , with most of the lower C_3 trajectories possible only when targeting a Haumea or Quaoar flyby. High performing type 2 trajectories prefer a perihelion of ~ 4 solar radii, and the ΔV at perihelion has a proffered value of around 6.8 km/sec.

Discrete launch opportunities exist over the whole 8-year launch period. KBOs MakeMake and Haumea prefer launches before or around the year 2025. Orcus is only accessible for launch dates near the end of year 2023. Trajectories to Quaoar prefer later launch dates between the years 2026 and early 2029.

Three-flyby trajectories: Figure 8 maps the trade space for type 2 trajectories with three solar-system flybys (two inner solar system flybys before Jupiter). These trajectories are generally inferior to the two-flyby trajectories in terms of V_∞^{sun} and distance achieved in 20 years while having similar launch C_3 requirements. The only benefit (over the two-flyby trajectories) offered by these trajectories is the flexibility in launch dates, especially when targeting a Quaoar flyby.

Four-flyby trajectories: Figure 9 maps the trade space for type 2 trajectories with four solar-system flybys. These trajectories are the best performing in terms of launch C_3 and V_∞^{sun} . Many of the four-flyby trajectories have low launch C_3 requirements, get close to 200 AU and achieve $V_\infty^{sun} > 13$ AU/yr. The flight to the KBO is ~ 11 years for high performing cases. Perihelion ΔV ranges from 4.7 to 7.8 km/sec with the sweet spot being around 7 km/sec. These trajectories also offer flexibility in launch dates when targeting KBOs Haumea and Quaoar.

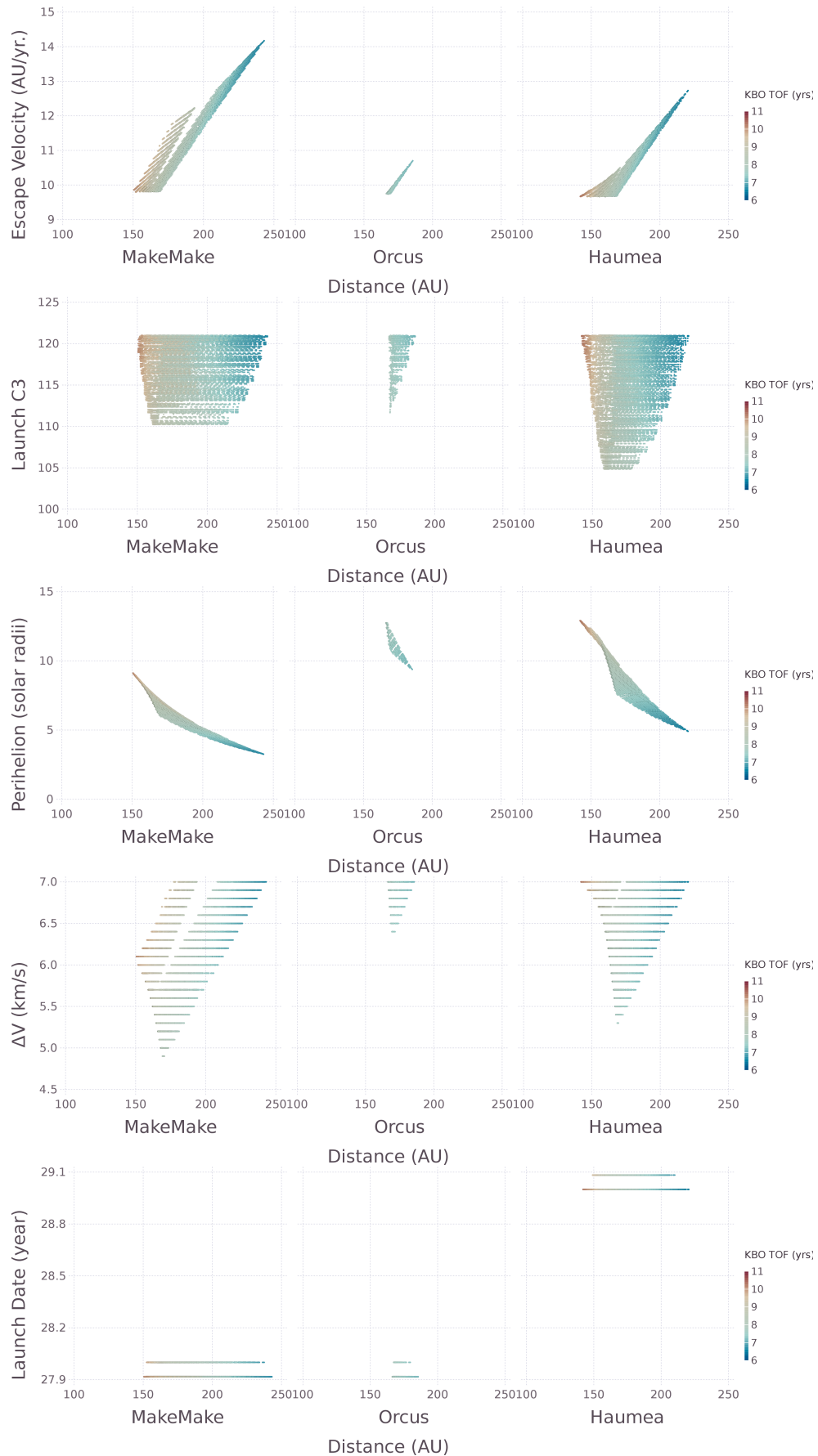


Figure 6. Results: Type 2 Trajectories (with a Jupiter flyby)

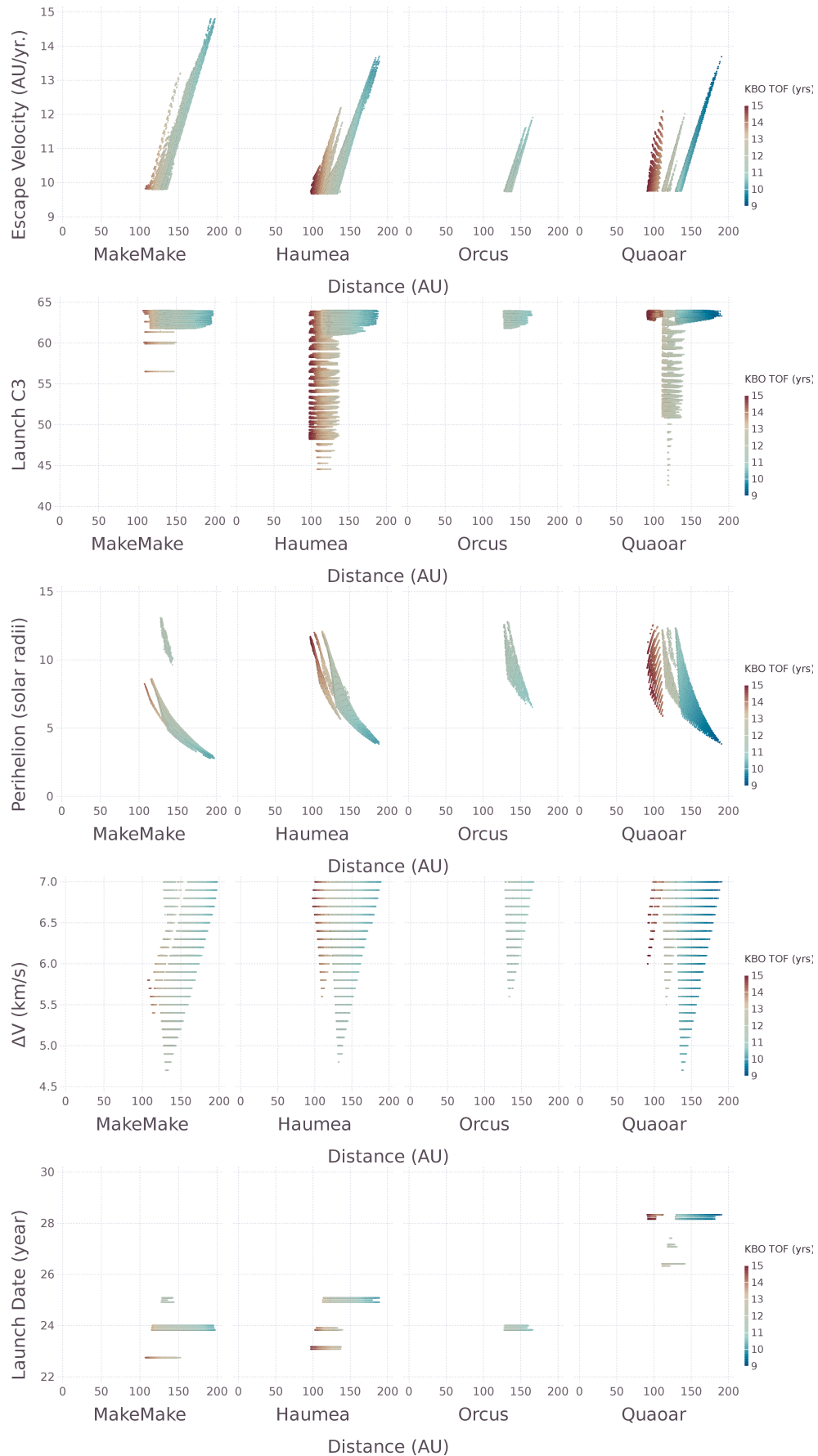


Figure 7. Results: Type 2 Trajectories (two inner planets (1+Jupiter) flybys)

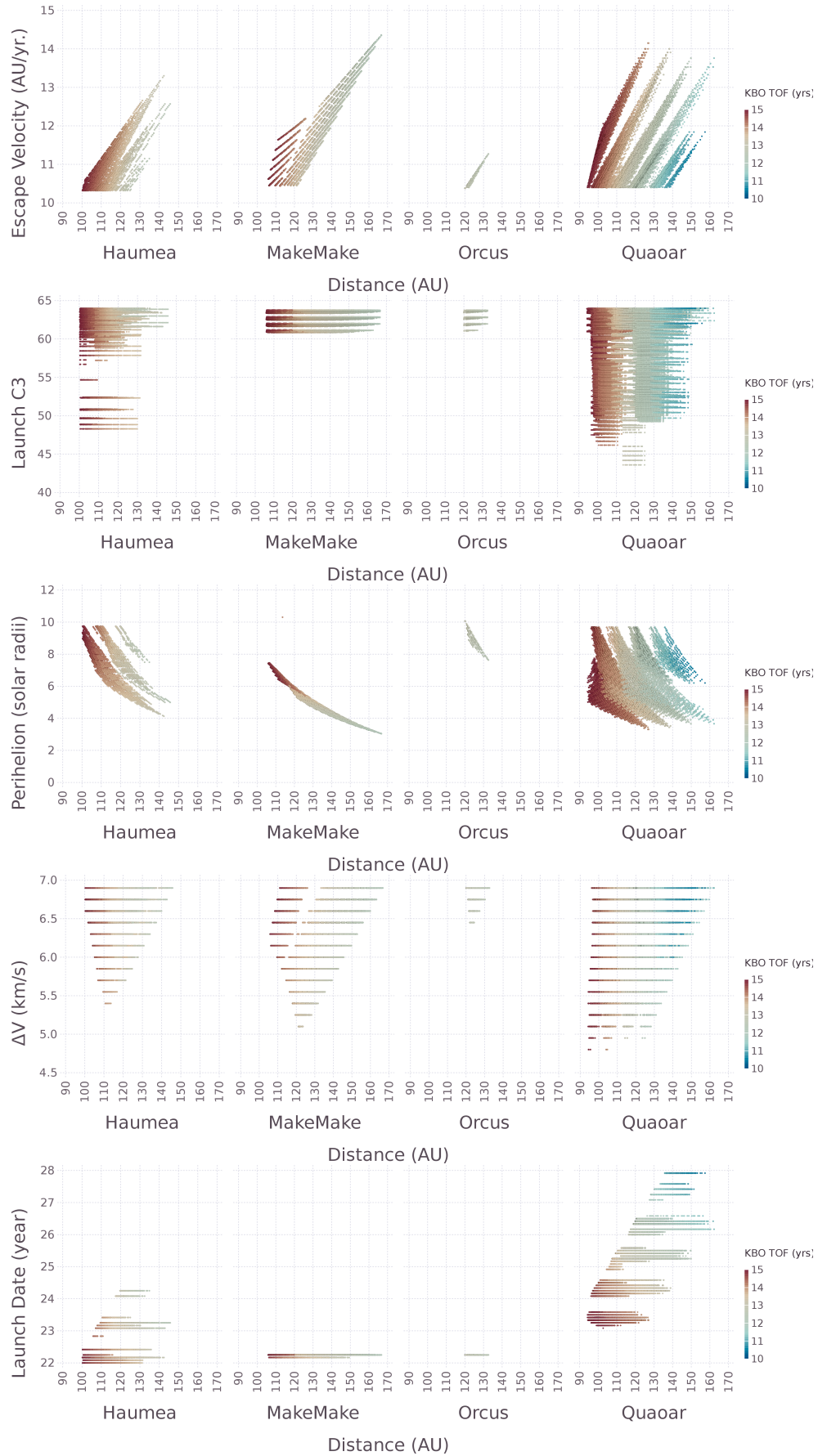


Figure 8. Results: Type 2 Trajectories (three inner planets (2+Jupiter) flybys)

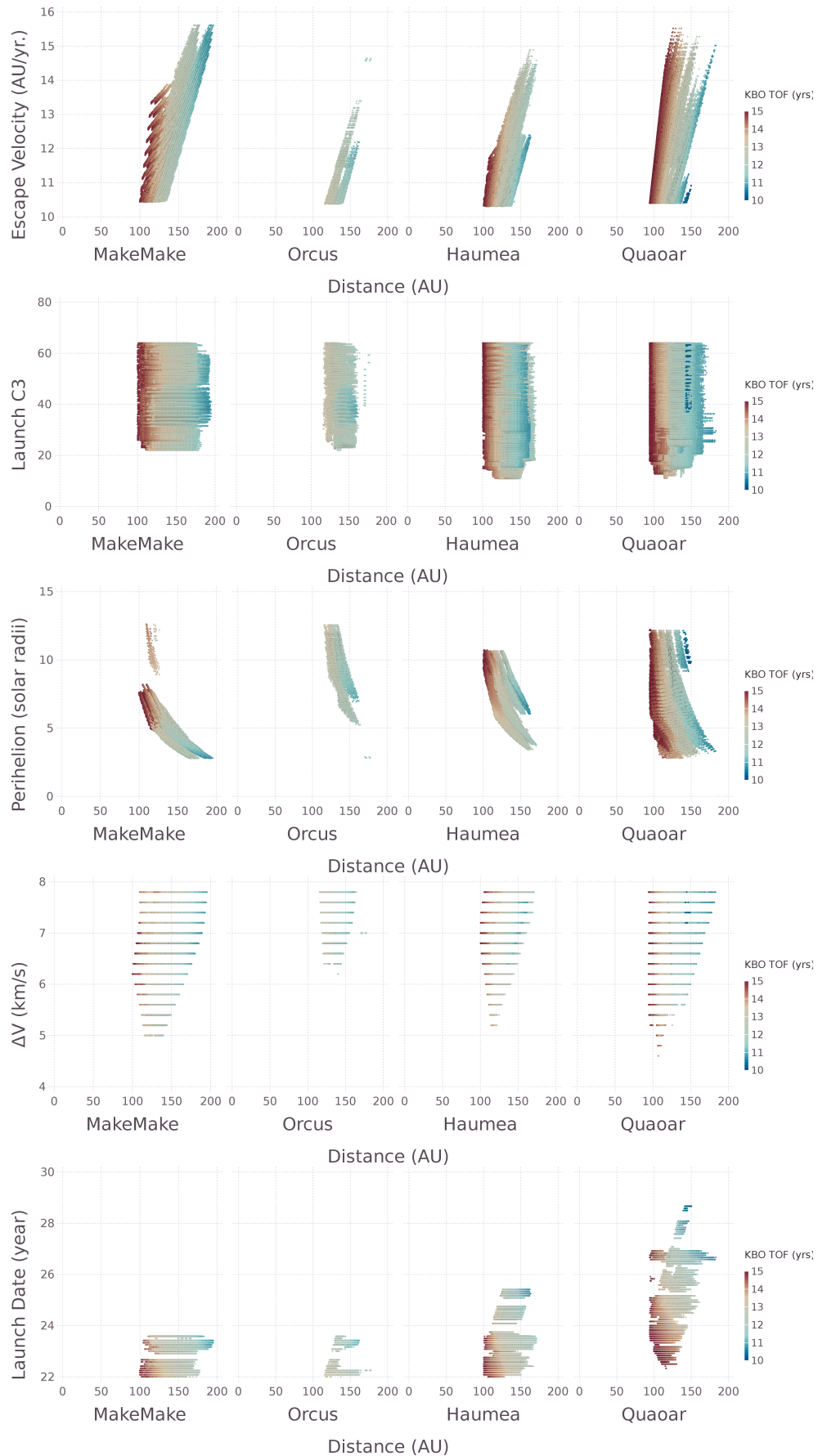


Figure 9. Results: Type 2 Trajectories (four inner planets (3+Jupiter) flybys)

Type 2 trajectories results summary: Table 5 lists the characteristics of the overall best trajectories for each KBO for various ranges of launch C_3 . Note that none of the inferior three-flyby type 2 trajectories are shown here. Figure 10 shows two optimized four-flyby trajectories (corresponding to cases 17 and 18 in table 5) to MakeMake (left) and Quaoar (right), respectively. Note that the MakeMake trajectory drops below the ecliptic plane after Jupiter flyby and has a near polar approach to the Sun. Hence, the perihelion burn vector has a large out-of-plane (Z direction) component. This is a direct result of MakeMake having an inclination of ~ 25 degrees.

Table 5. Some representative Type 2 Trajectories(unoptimized)

| Case | KBO | Flybys (inner solar system) | Launch (month/year) | Flyby Dates (month/year) | KBO TOF (yrs) | Distance (AU) | V_{∞}^{sun} (AU/yr) | C_3 (km^2/s^2) | Perihelion Radii, ΔV (solar radii, km/sec) |
|--|----------|--------------------------------|------------------------|-----------------------------|------------------|------------------|-------------------------------|---------------------------------------|---|
| $C_3 \geq 100 \text{ km}^2/\text{s}^2$ | | | | | | | | | |
| 1 | MakeMake | J | 11/27 | 04/29 | 6.6 | 243 | 14.2 | 121 | 3.3,7.0 |
| 2 | Haumea | J | 12/28 | 04/30 | 6.5 | 221 | 12.7 | 121 | 4.9,7.0 |
| 3 | Orcus | J | 11/27 | 04/29 | 7.1 | 186 | 10.7 | 121 | 9.4,7.0 |
| $C_3 \leq 100 \text{ km}^2/\text{s}^2$ | | | | | | | | | |
| 4 | MakeMake | E,J | 10/23 | 12/27,3/29 | 10.2 | 197 | 14.8 | 64 | 2.8,7.0 |
| 5 | Haumea | E,J | 11/24 | 1/29,3/30 | 10 | 189 | 13.7 | 64 | 3.8,7.0 |
| 6 | Quaoar | E,J | 04/28 | 3/32,5/33 | 9.2 | 191 | 13.7 | 63 | 3.8,7.0 |
| 7 | Orcus | V,V,E,J | 03/22 | 3/23,3/24,12/26,4/28 | 11.5 | 178 14.7 | 59 | 2.8,7.0 | |
| $C_3 \leq 50 \text{ km}^2/\text{s}^2$ | | | | | | | | | |
| 8 | MakeMake | V,V,E,J | 5/23 | 8/23,1/25,1/28,4/29 | 10.9 | 195 | 15.6 | 41 | 2.8,7.8 |
| 9 | Haumea | V,E,E,J | 6/23 | 7/24,9/25,1/29,4/30 | 11.5 | 171 | 14.5 | 45 | 3.8,7.8 |
| 10 | Orcus | V,V,E,J | 3/22 | 3/23,3/24,12/26,4/28 | 11.5 | 172 | 14.6 | 49 | 2.8,7.0 |
| $C_3 \leq 30 \text{ km}^2/\text{s}^2$ | | | | | | | | | |
| 11 | MakeMake | V,V,E,J | 5/23 | 6/24,7/25,1/28,5/29 | 11.2 | 183 | 14.8 | 30 | 3.2,7.6 |
| 12 | Haumea | V,E,E,J | 8/22 | 6/24,10/25,1/29,5/30 | 13.2 | 129 | 11.7 | 11 | 5.7,6.4 |
| 13 | Quaoar | V,E,E,J | 8/26 | 5/28,6/28,2/32,5/33 | 10.6 | 183 | 15 | 30 | 3.3,7.8 |
| 14 | Orcus | V,E,E,J | 1/22 | 7/22,12/23,12/27,3/29 | 12.2 | 148 | 12.2 | 24 | 6.6,7.4 |
| $V_{\infty}^{sun} \sim 13 \text{ AU/Yr}$ | | | | | | | | | |
| 17 | MakeMake | V,V,E,J | 4/23 | 8/23,1/25,1/28,3/29 | 11 | 176 | 13.7 | 33 | 3.2, 6.4 |
| 18 | Quaoar | V,E,E,J | 8/26 | 5/28,6/28,2/32,5/33 | 11 | 168 | 13.7 | 31 | 3.8, 7.0 |

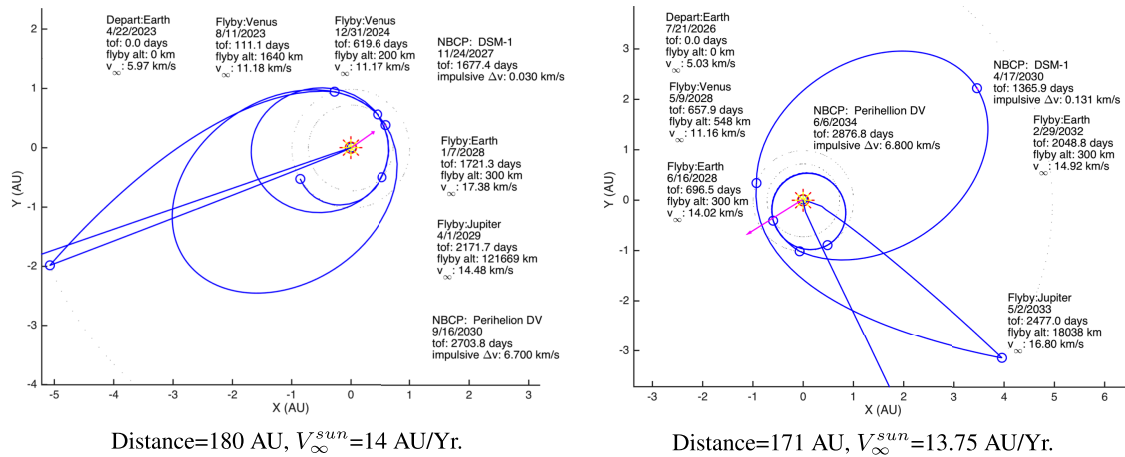


Figure 10. Trajectories to the ISM for MakeMake (left) and Quaoar (right)

Effect of Solar sail on Type 2 Trajectories

In this section we investigate possible performance improvements (increased escape velocity and reduced flight times) by deploying a solar sail on the escape leg of type 2 trajectories. To maximize the gain in velocity, the sail must be oriented such that the component of thrust is maximized along the velocity vector. The optimal sail orientation can be derived analytically and results in a simple feedback control law:

$$\theta = \frac{1}{2} \left[\phi + \arccos \left(\frac{\cos(\phi)}{3} \right) \right] \quad (2)$$

$$\hat{\mathbf{u}} = \cos(\theta) \hat{\mathbf{r}} + \sin(\theta) \hat{\mathbf{w}} \quad (3)$$

$$\hat{\mathbf{f}} = (\hat{\mathbf{u}} \cdot \hat{\mathbf{r}})^2 \hat{\mathbf{r}} \quad (4)$$

where θ is the angle between sail normal vector ($\hat{\mathbf{u}}$) and the sun-spacecraft vector ($\hat{\mathbf{r}}$), and ϕ is the angle between spacecraft velocity vector $\hat{\mathbf{v}}$ and the vector $\hat{\mathbf{w}}$, perpendicular to $\hat{\mathbf{r}}$ and in the plane spanned by $\hat{\mathbf{r}}$ and $\hat{\mathbf{v}}$. The sail acceleration is given as:

$$\vec{a}_{sail} = \left[\eta \frac{2AW}{cM_p} \right] \left(\frac{AU}{r} \right)^2 \hat{\mathbf{r}} \quad (5)$$

where A , W , η , r , c correspond to sail area, solar flux at 1 AU (a constant), sail efficiency parameter (assumed as unity for this study), distance between Sun and the spacecraft, and the speed of light, respectively. Orienting the sail according to the above control law, instead of in the direction of velocity, results in 5–7% improvement in sail performance.

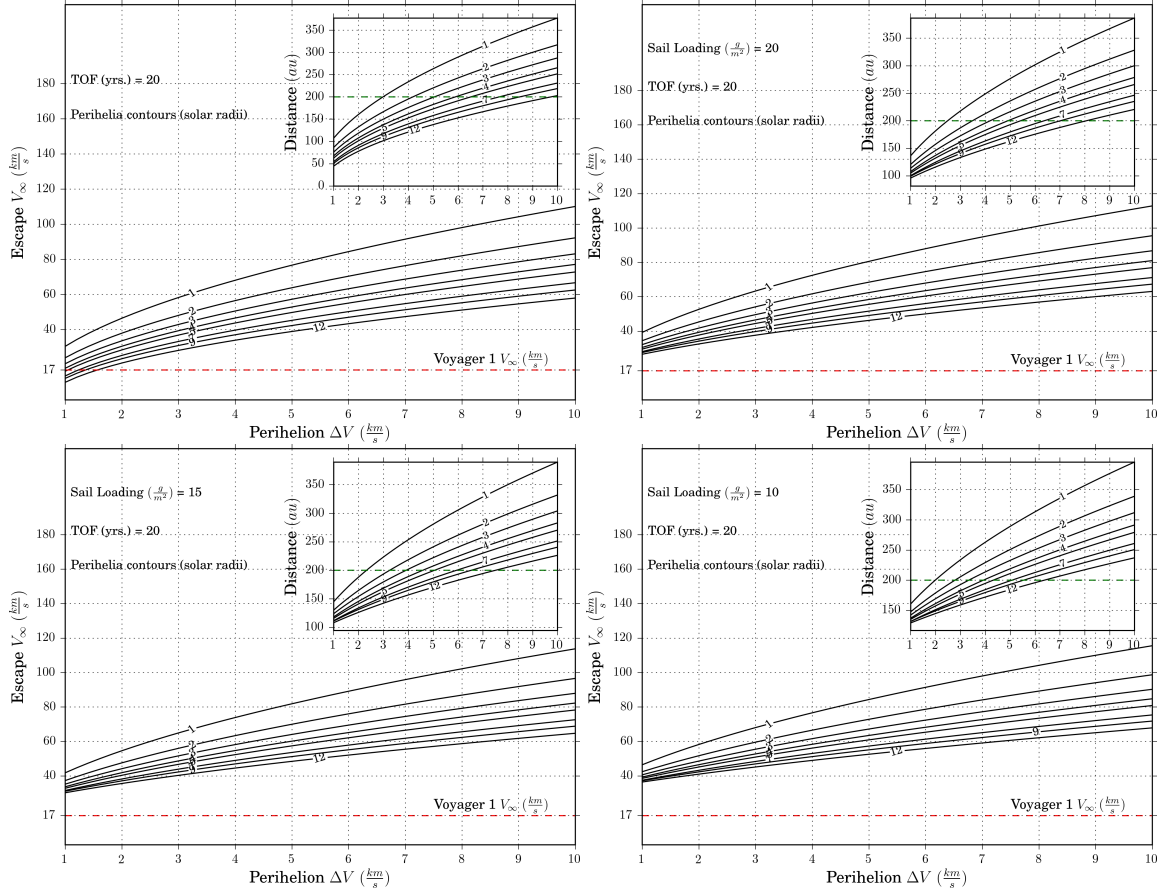


Figure 11. Solar sail performance benefit on a type 2 trajectory without a KBO targeting constraint. Top left = no sail, Sail loading (g/m^2) = 20(top right), 15(bottom left) and 10(bottom right).

For this study, the solar sail is assumed to be flat, perfectly reflective, non-ablative with a minimum sail deployment radial distance of 0.2 AU. The thin solar sail material is not expected to survive close to the Sun. Furthermore, the current analysis is restricted to type 2 trajectories with a single Jupiter flyby and without a KBO encounter on the escape leg. Finally, as stated in previous section, three values of sail loading (10, 15, and 20 g/m^2) are considered in this study. Figure 11 compares the impulsive-only case with the three solar sail cases corresponding to the three sail loading values. Each figure shows escape velocity V_{∞}^{sun} and distance after 20 years (from launch) as a function of perihelion ΔV for different perihelion radii. Even with an optimistic sail loading of 10 g/m^2 , only a small delta (~ 1 AU/yr improvement in escape speed) increase in trajectory performance is observed. Going to even lower sail loadings will result in more benefit from using

the sail, but will also most likely result in a complex engineering and navigation challenge. One possible benefit, which has not been investigated in this study, is the increased launch window, possible by using the sail on the escape leg to also target a KBO.

CONCLUSION

An exhaustive set of trajectories for a near-term (launch between 2022 and 2030) notional mission to the ISM with a KBO flyby are found and documented. Primary mission concept design drivers are: 1) reaching a distance of 180–200 AU in 20 years from launch and 2) escaping the solar system with a speed of >13 AU/yr. Based on the science objectives, four KBO candidates (MakeMake, Haumea, Quaoar, and Orcus) are identified for a KBO flyby.

An impulsive broad-search algorithm capable of adding resonant transfers, deep space maneuvers, and powered Oberth flybys is combined with a local pruning and optimization strategy to find the large set of feasible trajectories. Two classes of trajectory are identified: Type 1, with a powered Jupiter flyby, and Type 2, with perihelion maneuver after a Jupiter flyby. Multiple inner-planet gravity assists and deep space maneuvers are found to significantly reduce launch C_3 requirements. Targeting a KBO is found to constrain the solution design space due to phasing constraints and inclination requirements.

Type 1 trajectories allow for quick access to the KBO and the nearby ISM but at best achieve a solar system escape velocity of only ~ 10 AU/yr (compared to 3.6 AU/yr for Voyager 1 and 2.5 AU/yr for New Horizons). Furthermore, all high-performing type 1 trajectories require high launch C_3 s and very large ΔV s at Jupiter ($\sim 9+$ km/s on average) which limits their applicability to an actual mission scenario. Type 1 trajectories with inner solar system flybys show a 50% reduction in launch C_3 but suffer in mission performance (escape speed and distance after 20 years).

Compared to type 1 trajectories, type 2 trajectories offer almost $1.5\times$ the performance in terms of solar system escape speeds, but require a challenging maneuver close to the Sun. Type 2 trajectories relying only on high launch C_3 (>100 km²/sec²), a Jupiter flyby, and a perihelion maneuver achieve solar system escape speeds of ~ 14 AU/yr and reach a distance of >200 AU in 20 years. Adding multiple inner-planet flybys (of Venus, Earth, or Mars) and deep-space maneuvers allows us to significantly reduce the launch C_3 requirements, by a factor of 4 in some cases, with a modest (1–3 years) increase in flight times to 200 AU. Adding an optimistically-designed solar sail (sail area of 30,000 m²) on the escape phase (without a KBO flyby) of a type 2 trajectory results in a $\sim 5\%$ increase in escape speed, but comes with added engineering and navigation complexity.

Future studies will look at investigating trajectories using low-thrust propulsion, electric sails, and trajectories with multiple KBO flybys. Given the high ΔV nature of this mission, future studies will also optimize the mission flight system and launch vehicle performance along with a baseline mission trajectory.

A near-term mission, as proposed in this work, would be humanity's first ever endeavor (either NASA or international) to explicitly target the local ISM as the next scientific frontier, and journey deep into the pristine ISM. The mission would be daring, challenging, and inspiring to the public and would be a rational first step before attempting to reach another star.

ACKNOWLEDGMENT

The research described in this paper was in part sponsored by the Caltech Keck Institute for Space Studies (KISS) and was carried out in part at the Jet Propulsion Laboratory, California Institute of Technology, under contract with the National Aeronautics and Space Administration. For long, fruitful discussions and insights, the authors acknowledge Robert J. Cesarone, one of the Voyager-2 navigators at JPL. The authors also acknowledge Daniel Grebow, member of the Outer Planets Mission Analysis group at JPL, for his help with the solar sail steering law.

REFERENCES

- [1] “Voyager 1 enters Interstellar space,” <http://www.jpl.nasa.gov/news/news.php?release=2013-278>. Accessed: Aug. 2015.
- [2] “New Horizons Pluto flyby,” <http://pluto.jhuapl.edu/News-Center/News-Article.php?page=20150714-4>. Accessed: Aug. 2015.
- [3] “NASA’s Kepler mission,” <http://kepler.nasa.gov/>. Accessed: Aug. 2015.
- [4] “KISS ISM Workshop,” <http://kiss.caltech.edu/study/science.html>. Accessed: Aug. 2015.
- [5] L. Alkalai, L. Friedman, and E. C. Stone, “Overview of the Keck Institute for Space Studies (KISS) Workshops on the Science and Enabling Technologies for the Exploration of the Interstellar Medium (ISM),” *66th International Astronautical Congress*, Jerusalem, Israel, October 2015.
- [6] L. Alkalai and N. Arora, “The Interstellar Medium (ISM) the Next Frontier in Space Science and Exploration,” *IAA Symposium on the Future of Space Exploration*, Torino, Italy, July 2015.
- [7] N. Arora, L. Alkalai, and N. Strange, “A Novel Mission Concept for Near Term Exploration of the Interstellar Medium,” *66th International Astronautical Congress*, Jerusalem, Israel, October 2015.
- [8] L. D. Jaffe, C. V. Ivie, J. C. Lewis, R. Lipes, H. N. Norton, and J. W. Stearns, “An interstellar precursor mission,” *J. Brit. Int. Soc.*, Vol. 33, 1980, pp. 3–26.
- [9] E. V. Pawlik and W. M. Phillips, “A nuclear electric propulsion vehicle for planetary exploration,” *J. Spacecraft*, Vol. 14, 1977, pp. 518–525.
- [10] R. A. Wallace, “Precursor missions to interstellar exploration,” *Aerospace Conference, Snowmass at Aspen, CO*, 1999, pp. 413–420.
- [11] P. C. Liewer, R. A. Mewaldt, J. A. Ayon, C. Gamer, S. Gavit, and R. A. Wallace, “Interstellar probe using a solar sail: Conceptual design and technological challenges,” *COSPAR Colloquium on The Outer Heliosphere: The Next Frontiers COSPAR Colloquia Series*, Vol. 11, 2001, pp. 411–420.
- [12] L. Johnson and S. Leifer, “Propulsion options for interstellar exploration,” *AIAA Paper*, Vol. 3334, 2000.
- [13] R. L. McNutt Jr, R. E. Gold, T. Krimigis, E. C. Roelof, M. Gruntman, G. Gloeckler, P. L. Koehn, W. S. Kurth, S. R. Oleson, D. I. Fiehler, *et al.*, “Innovative interstellar explorer,” 2006.
- [14] D. Routier, “A Solar-Ion Propelled Mission to the Local Interstellar Medium,” *Journal of the British Interplanetary Society*, Vol. 49, No. 5, 1996, p. 193.
- [15] R. Mcdutt, “A sole/ad astra: From the Sun to the stars,” *Journal of the British Interplanetary Society*, Vol. 50, No. 12, 1997, pp. 463–474.
- [16] F. J. Dyson, “Interstellar transport,” *Physics Today*, Vol. 21, No. 10, 1968, pp. 41–45.
- [17] R. Lyman, M. Ewing, R. Krishnan, D. Lester, and J. Ralph McNutt, “Solar thermal propulsion for an interstellar probe,” *Joint Propulsion Conferences*, American Institute of Aeronautics and Astronautics, July 2001, 10.2514/6.2001-3377.
- [18] D. I. Fiehler and R. L. McNutt, “Mission design for the innovative interstellar explorer vision mission,” *Journal of spacecraft and rockets*, Vol. 43, No. 6, 2006, pp. 1239–1247.
- [19] M. Leipold, H. Fichtner, B. Heber, P. Groepper, S. Lascar, F. Burger, M. Eiden, T. Niederstadt, C. Sickinger, L. Herbeck, *et al.*, “Heliopause explorer sailcraft mission to the outer boundaries of the solar system,” *Acta Astronautica*, Vol. 59, No. 8, 2006, pp. 785–796.
- [20] V. Lappas, M. Leipold, A. Lyngvi, P. Falkner, H. Fichtner, and S. Kraft, “Interstellar heliopause probe: system design of a Solar Sail mission to 200 AU,” *AIAA Guidance, Navigation, and Control Conference and Exhibit, AIAA Paper*, Vol. 6084, 2005, pp. 15–18.
- [21] R. F. Wimmer-Schweingruber, R. L. McNutt Jr, *et al.*, “The Interstellar Heliopause Probe/Heliospheric Explorer: IHP/HEX,” *Twelfth International Solar Wind Conference*, Vol. 1216, AIP Publishing, 2010, pp. 655–658.
- [22] R. L. McNutt Jr, M. S. Elsperman, M. Gruntman, K. K. Klaus, S. M. Krimigis, and e. a. E. C. Roelof, “Enabling Interstellar Probe with the Space Launch System (SLS),” 2014.
- [23] R. Mewaldt, J. Kangas, S. Kerridge, and M. Neugebauer, “A small interstellar probe to the heliospheric boundary and interstellar space,” *Acta Astronautica*, Vol. 35, 1995, pp. 267–276.
- [24] D. McComas, F. Allegrini, P. Bochsler, M. Bzowski, E. Christian, G. Crew, R. DeMajistre, H. Fahr, H. Fichtner, P. Frisch, *et al.*, “Global observations of the interstellar interaction from the Interstellar Boundary Explorer (IBEX),” *Science*, Vol. 326, No. 5955, 2009, pp. 959–962.
- [25] N. V. Pogorelov, G. P. Zank, and T. Ogino, “Three-dimensional features of the outer heliosphere due to coupling between the interstellar and interplanetary magnetic fields. II. The presence of neutral hydrogen atoms,” *The Astrophysical Journal*, Vol. 644, No. 2, 2006, p. 1299.

- [26] H. Funsten, F. Allegrini, G. Crew, R. DeMajistre, P. Frisch, S. Fuselier, M. Gruntman, P. Janzen, D. McComas, E. Möbius, *et al.*, “Structures and spectral variations of the outer heliosphere in IBEX energetic neutral atom maps,” *Science*, Vol. 326, No. 5955, 2009, pp. 964–966.
- [27] W. Groesbeck, “Centaur Upper Stage,” *Orbital Debris from Upper Stage Breakup*, Vol. 121, 1989, p. 211.
- [28] H. Oberth, *Ways to spaceflight*. No. 622, National Aeronautics and Space Administration, 1972.
- [29] Y. Guo, “Trajectory design of Solar Probe+ using multiple Venus gravity assists,” *AIAA Paper*, Vol. 7365, 2008, p. 2008.
- [30] Y. Guo and R. W. Farquhar, “Current mission design of the solar probe mission,” *Acta Astronautica*, Vol. 55, No. 3, 2004, pp. 211–219.
- [31] E. A. Rinderle, “Galileo Users Guide, Mission Design System, Satellite Tour Analysis and Design Subsystem,” *Jet Propulsion Laboratory, California Institute of Technology, Pasadena, CA, JPL D-263*, 1986.
- [32] D. Lantukh and R. P. Russell, “Multi-Objective Search for Multiple Gravity Assist Trajectories,” *AAS/AIAA Astrodynamics Specialist Conference*, Vail, CO, 2015.
- [33] D. Landau, “Efficient Maneuver Placement for Automated Trajectory Design,” *AAS/AIAA Astrodynamics Specialist Conference*, Vail, CO, 2015.
- [34] D. F. Lawden, *Optimal trajectories for space navigation*. Butterworths, 1963.
- [35] F. W. Gobetz, “Optimum transfers between hyperbolic asymptotes,” *AIAA Journal*, Vol. 1, No. 9, 1963, pp. 2034–2041.
- [36] J. M. Walton, C. Marchal, and R. D. Culp, “Synthesis of the types of optimal transfers between hyperbolic asymptotes,” *AIAA Journal*, Vol. 13, No. 8, 1975, pp. 980–988.
- [37] R. A. Hyde, *Trajectory optimization involving powered planetary swingbys*. PhD thesis, Massachusetts Institute of Technology, 1973.
- [38] J. A. Sims, P. A. Finlayson, E. A. Rinderle, M. A. Vavrina, and T. D. Kowalkowski, *Implementation of a low-thrust trajectory optimization algorithm for preliminary design*. Pasadena, CA: Jet Propulsion Laboratory, National Aeronautics and Space Administration, 2006.
- [39] J. Bezanson, S. Karpinski, V. B. Shah, and A. Edelman, “Julia: A Fast Dynamic Language for Technical Computing,” *ArXiv e-prints*, Sept. 2012.